Nuclear receptors PPARβ/δ and PPARα direct distinct metabolic regulatory programs in the mouse heart

Eileen M. Burkart,[1,2] Nandakumar Sambandam,[1,2] Xianlin Han,[2]
Richard W. Gross,[2,3] Michael Courtois,[1,2] Carolyn M. Gierasch,[1,2]
Kooresh Shoghi,[3,4] Michael J. Welch,[3,4] and Daniel P. Kelly[1,2,3,5]

[1]Center for Cardiovascular Research, [2]Department of Medicine, [3]Department of Molecular Biology and Pharmacology,
[4]Department of Radiology, and [5]Department of Pediatrics, Washington University School of Medicine, St. Louis, Missouri, USA.

In the diabetic heart, chronic activation of the PPARα pathway drives excessive fatty acid (FA) oxidation, lipid accumulation, reduced glucose utilization, and cardiomyopathy. The related nuclear receptor, PPARβ/δ, is also highly expressed in the heart, yet its function has not been fully delineated. To address its role in myocardial metabolism, we generated transgenic mice with cardiac-specific expression of PPARβ/δ, driven by the myosin heavy chain (MHC-PPARβ/δ mice). In striking contrast to MHC-PPARα mice, MHC-PPARβ/δ mice had increased myocardial glucose utilization, did not accumulate myocardial lipid, and had normal cardiac function. Consistent with these observed metabolic phenotypes, we found that expression of genes involved in cellular FA transport were activated by PPARα but not by PPARβ/δ. Conversely, cardiac glucose transport and glycolytic genes were activated in MHC-PPARβ/δ mice, but repressed in MHC-PPARα mice. In reporter assays, we showed that PPARβ/δ and PPARα exerted differential transcriptional control of the GLUT4 promoter, which may explain the observed isotype-specific effects on glucose uptake. Furthermore, myocardial injury due to ischemia/reperfusion injury was significantly reduced in the MHC-PPARβ/δ mice compared with control or MHC-PPARα mice, consistent with an increased capacity for myocardial glucose utilization. These results demonstrate that PPARα and PPARβ/δ drive distinct cardiac metabolic regulatory programs and identify PPARβ/δ as a potential target for metabolic modulation therapy aimed at cardiac dysfunction caused by diabetes and ischemia.

Introduction

We are witnessing a pandemic of obesity-related diabetes (1). Diabetes predisposes to heart failure, particularly in combination with other comorbid conditions such as hypertension and coronary artery disease (2, 3). The incidence of heart failure and death following myocardial infarction is higher in diabetic than in nondiabetic individuals (4–9). Evidence is emerging that derangements in cardiac fuel metabolism, related to insulin resistant and diabetic states, contribute to the development of diabetic cardiac dysfunction. The normal adult heart satisfies its energy requirements through the oxidation of both fatty acids (FAs) and glucose (10, 11). However, myocardial insulin resistance and increased rates of systemic lipolysis force the diabetic heart to rely almost exclusively on FA as a fuel source, a loss of substrate flexibility (12–14). Over the long term, high rates of myocardial FA utilization predispose to the development of a "lipotoxic" form of cardiomyopathy, characterized by myocyte lipid accumulation, mitochondrial dysfunction, and generation of reactive oxygen species related to excessive substrate flux (12–16). In addition, the diabetic heart has a reduced capacity for glycolysis and glucose oxidation, which predisposes to postischemic damage (17, 18).

Recent evidence has implicated dysregulation of the nuclear receptor PPARα (Ppara) in the metabolic and functional derangements of the diabetic heart (19, 20). PPARα activates transcription of genes involved in cellular lipid utilization pathways, including FA uptake and FA oxidation (FAO) (21, 22). The PPARα gene regulatory pathway is chronically activated in the hearts of insulin-deficient and insulin-resistant rodents (19). Transgenic mice with cardiac-specific overexpression of PPARα (MHC-PPARα mice) display a functional and metabolic phenotype that mimics the diabetic heart (19). Specifically, MHC-PPARα mouse hearts exhibit increased FAO rates, decreased glucose utilization, myocyte triacylglyceride (TAG) accumulation, and cardiomyopathy. Interestingly, the lipotoxic cardiomyopathy of MHC-PPARα mice is worsened with consumption of a high-fat (HF) diet (20). Consistent with observations in animal models, recent studies using PET have shown that hearts of diabetic humans exhibit increased FA uptake and utilization rates (19, 23, 24).

PPARα is a member of a FA-activated nuclear receptor family that includes PPARγ (Pparg) and PPARβ/δ (Ppard) (21). In contrast to PPARγ, which is adipose enriched, PPARβ/δ is highly expressed in cardiac myocytes, similar to PPARα (25). Whereas the function of PPARα has been the subject of intense investigation, less is known about PPARβ/δ. Mice with cardiac-specific deletion of the PPARβ/δ gene were recently shown to develop myocardial lipid accumulation and cardiomyopathy (26). These results suggest that PPARβ/δ is necessary for myocardial lipid homeostasis. However, the biologic response and corresponding gene activation profiles following activation of the PPARβ/δ pathway, compared with PPARα, have not been fully delineated.

A

B
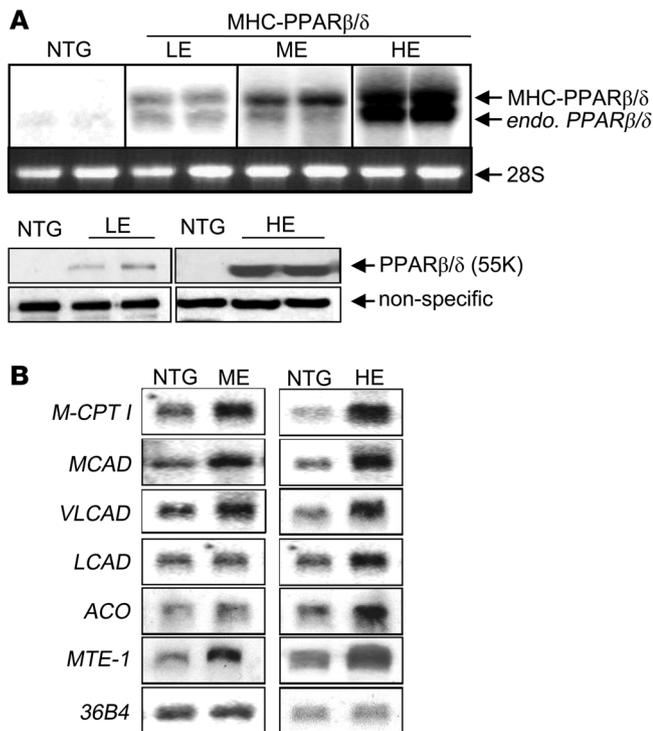
Figure 1
Generation of MHC-PPARβ/δ mice. (**A**) Top: Representative autoradiographs of Northern blot analyses performed with RNA isolated from hearts of 8-week-old mice from independent MHC-PPARβ/δ–LE, MHC-PPARβ/δ–ME, and MHC-PPARβ/δ–HE lines. At the exposure shown, endogenous (endo) PPARβ/δ was not detected in NTG samples. Note that the endogenous PPARβ/δ transcript was induced in the transgenic heart (lower band). The 28s rRNA is shown as a loading control. Bottom: Representative Western blots performed with protein isolated from cardiac ventricles of MHC-PPARβ/δ–LE and MHC-PPARβ/δ–HE mice. The nonspecific signal is shown as a control for loading. (**B**) Representative Northern blot showing the expression of known PPARα target genes in hearts of MHC-PPARβ/δ–ME and MHC-PPARβ/δ–HE mice. The *36B4* signal is shown as a loading control.

To investigate the role of PPARβ/δ in the regulation of heart metabolism and function, we generated and characterized transgenic mice with cardiac-specific expression of PPARβ/δ (MHC-PPARβ/δ mice). Surprisingly, in contrast to MHC-PPARα mice, MHC-PPARβ/δ mice did not develop cardiomyopathy and exhibited a strikingly different cardiac fuel preference. This PPAR isotype–specific response was also observed following ligand-mediated activation of the endogenous nuclear receptors. The PPAR-specific effects on cardiac metabolism were dictated by both shared and distinct gene targets. Most notably, PPARβ/δ activated, whereas PPARα repressed, targets involved in the cellular glucose utilization pathway. Our results suggest that one mechanism whereby PPARβ/δ and PPARα exert reciprocal effects on cellular glucose uptake occurs through differential regulation of glucose transporter 4 (*GLUT4*; *Slc2a4*) gene transcription.

Results

Generation of MHC-PPARβ/δ mice. To explore the effects of PPARβ/δ in the heart, we generated transgenic mice with cardiac-specific expression of PPARβ/δ. Three independent lines of MHC-PPARβ/δ mice were established, with varying levels of transgene expression — from high physiologic to supraphysiologic — compared with endogenous PPARβ/δ; these were designated low, medium, and high expression (LE, ME, and HE, respectively; Figure 1A). The lines of MHC-PPARβ/δ mice were chosen so that the range of transgene expression overlapped with that of MHC-PPARα lines generated previously; approximately 20-fold (MHC-PPARβ/δ–LE), 50-fold (MHC-PPARβ/δ–ME), and 100-fold (MHC-PPARβ/δ–HE) over levels of the corresponding endogenous nuclear receptor (ref. 19 and data not shown). MHC-PPARβ/δ transgene expression was confined to the heart (data not shown). MHC-PPARβ/δ mice were viable, born in the expected Mendelian ratios, and appeared normal.

The expression of known cardiac PPARα target genes was characterized in hearts of MHC-PPARβ/δ mice compared with nontransgenic (NTG) littermates. The levels of mRNA encoding muscle carnitine palmitoyltransferase Ib (M-CPT 1b; Cpt1b), which catalyzes the rate-limiting step of mitochondrial import of long-chain FAs, was induced in MHC-PPARβ/δ–ME and MHC-PPARβ/δ–HE mice (Figure 1B). In addition, expression of PPARα target genes involved in *mitochondrial* (medium-, long-, and very long-chain acyl-Coenzyme A dehydrogenase [*MCAD, Acadm*; *LCAD, Acadl*; and *VLCAD, Acadvl*, respectively]) and *peroxisomal* (acyl-Coenzyme A oxidase [*ACO*; *Acox1*]) FAO and FA dethioesterification (mitochondrial thioesterase 1 [*MTE-1*; *Mte1*]) was significantly higher in MHC-PPARβ/δ–ME and MHC-PPARβ/δ–HE mice than in controls (Figure 1B). However, only a subset of PPARα target genes (*MCAD, ACO*, and *MTE-1*) were found to be significantly upregulated in the MHC-PPARβ/δ–LE mice (data not shown).

MHC-PPARβ/δ mice do not develop lipotoxic cardiomyopathy. MHC-PPARα mice develop cardiac hypertrophy and dysfunction in association with myocardial lipid accumulation and high FA uptake and utilization rates (19), a phenotype that resembles the diabetic heart. Hearts from 8-week-old, sex-matched MHC-PPARα and MHC-PPARβ/δ mice and corresponding NTG littermates were examined for signs of ventricular hypertrophy and cardiac dysfunction. As shown previously, the mean biventricular wt/body wt ratio of MHC-PPARα hearts was significantly greater than that of controls (3.9 ± 0.2 versus 3.3 ± 0.1; *P* < 0.05), even at low levels of transgene expression. In contrast, MHC-PPARβ/δ mice did not exhibit cardiac hypertrophy at any level of transgene expression (Supplemental Figure 1A; supplemental material available online with this article; doi:10.1172/JCI32578DS1). Similar results were obtained whether the ventricular weights were normalized to body weight or tibia length (Supplemental Figure 1B).

Echocardiography was performed to assess cardiac function of MHC-PPARβ/δ mice. On standard chow, LV fractional shortening (FS) was modestly but significantly decreased in MHC-PPARα–LE mice (50.7% ± 5.4%) compared with controls (58.5% ± 6.7%; *P* < 0.05; Figure 2 and Supplemental Table 1). As expected, an 8-week course of HF diet (43% of total calories as fat) resulted in severe cardiac dysfunction in MHC-PPARα–LE mice, manifest as a significant decline in LV FS (41.1% ± 5.9%) compared with controls (63.2% ± 5.2%; *P* < 0.01; Figure 2) as well as systolic and diastolic ventricular dilatation (Supplemental Table 1). In striking contrast, MHC-PPARβ/δ–LE mice did not exhibit any evidence of ventricular dysfunction or abnormal chamber enlargement
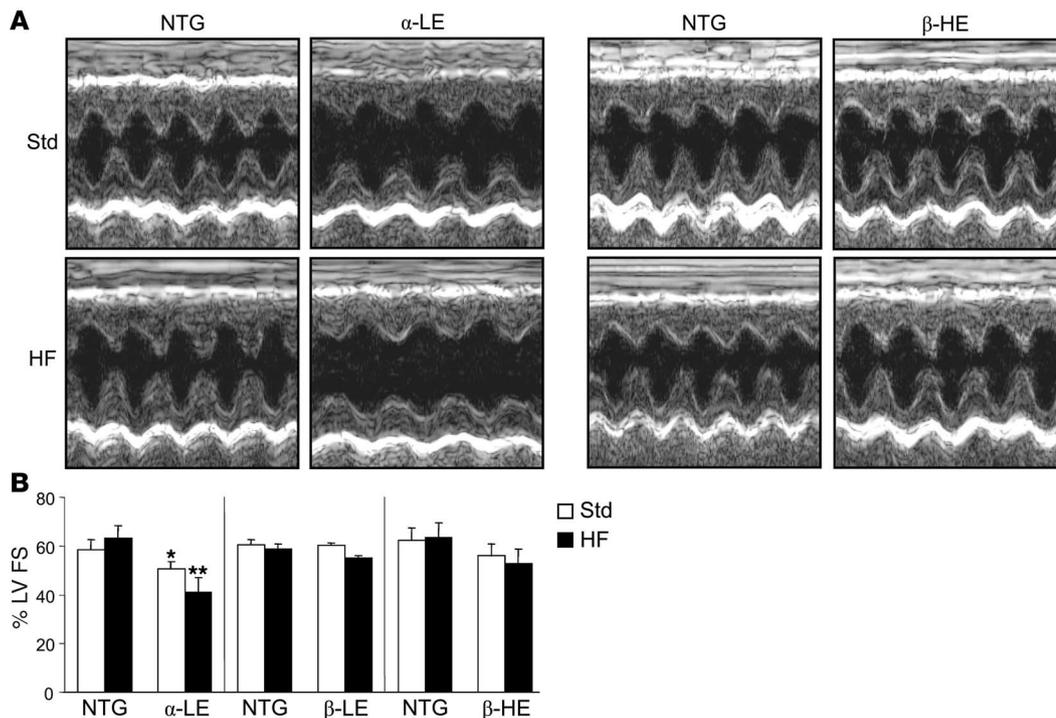
Figure 2
Cardiomyopathy develops in MHC-PPARα mice, but not MHC-PPARβ/δ mice. (**A**) Representative M-mode echocardiographic images of the LV of 8-week-old male MHC-PPARβ/δ–HE and MHC-PPARα–LE mice and NTG littermates after standard (Std) or HF diet treatment. (**B**) Mean percent LV FS ($n \geq 7$ per group) as assessed by echocardiographic analysis. *$P < 0.05$ versus NTG; **$P < 0.05$ versus NTG and standard diet–treated MHC-PPARα–LE.

on standard or HF diets (Figure 2 and Supplemental Table 1). This latter observation held true even in the MHC-PPARβ/δ–HE transgenic line (Figure 2).

The absence of a cardiomyopathic phenotype in the MHC-PPARβ/δ mice led us to explore the metabolic signatures of lipotoxicity. MHC-PPARβ/δ and MHC-PPARα mice were fed HF chow for 8 weeks or fasted for 48 hours (to rapidly increase circulating nonesterified FAs). Levels of myocardial neutral fat were visualized semiquantitatively by oil red O staining, followed by characterization and quantification of TAG species using electrospray ionization mass spectrometry (ESI/MS). In contrast to MHC-PPARα mice, MHC-PPARβ/δ hearts did not accumulate abnormal levels of neutral lipid (Figure 3A). Similar results were obtained following a 48-hour fast (data not shown). Quantification of TAG levels by ESI/MS demonstrated a significant increase in myocardial TAG levels in MHC-PPARα mice given HF diet or following a 48-hour fast compared with controls (Figure 3A). In striking contrast, no significant difference in myocardial TAG levels was observed in MHC-PPARβ/δ mice compared with controls following HF diet or fasting. Taken together with the echocardiographic data, these results demonstrate that, in contrast to MHC-PPARα mice, MHC-PPARβ/δ mice do not develop lipotoxic cardiomyopathy.

Previously, we have shown that neutral lipid accumulation within the myocytes of MHC-PPARα hearts is associated with activation of target genes involved in cellular FA uptake and TAG synthesis. Therefore, we sought to determine whether these gene regulatory programs were activated in the MHC-PPARβ/δ mice, given the lack of an observed myocardial lipid phenotype. Expression of genes involved in cellular FA transport was significantly upregulated in MHC-PPARα–LE mice, including FA transport protein–1 (*FATP-1*; *Slc27a1*; 2.42-fold ± 0.09-fold) and *CD36* (*Cd36*) (2.13-fold ± 0.09-fold; Figure 3B). In addition, the expression of genes encoding several key TAG synthesis and lipogenic enzymes, including glycerol-phosphate-3-acyl transferase (GPAT; *Gpam*),

acyl-Coenzyme A synthase (ACS; *Acsl1*), and FA synthase (FAS; *Fasn*), was increased in the hearts of MHC-PPARα mice compared with controls (Figure 3B). The expression of the microsomal transfer protein (*MTP*; *Mttp*) gene was also markedly increased in the MHC-PPARα hearts, presumably as a homeostatic response to export excess lipid as lipoprotein. In contrast, expression of the FA uptake, lipogenic, and TAG synthesis gene regulatory programs was not activated in MHC-PPARβ/δ–HE mouse hearts, with the exception of a modest increase in MTP mRNA levels. These results suggest that the abnormal TAG accumulation in MHC-PPARα mice, but not in MHC-PPARβ/δ mice, is related to differential activation of gene regulatory programs involved in FA uptake and TAG synthesis in the former, despite activation of genes involved in mitochondrial and peroxisomal FAO in both lines (Figure 1B).

MHC-PPARβ/δ mice exhibit increased myocardial glucose uptake and utilization rates. The hallmarks of metabolic derangements of the diabetic heart include reduced glucose uptake and utilization, concomitant with increased FA utilization, a fuel utilization profile that is recapitulated in MHC-PPARα mice (19, 27). To assess myocardial fuel utilization in MHC-PPARβ/δ mice, microPET studies were performed using 1-^{11}C-glucose and ^{11}C-palmitate as tracers. Surprisingly, rates of myocardial glucose uptake were significantly increased in MHC-PPARβ/δ–HE mice, whereas ^{11}C-palmitate in MHC-PPARβ/δ–HE mice was not different compared with controls (Figure 4A). Substrate oxidation rates were determined in working hearts isolated from MHC-PPARβ/δ–HE mice and NTG controls using [9,10-^{3}H]palmitate and [U-^{14}C]glucose. Consistent with the microPET results, glucose oxidation rates were significantly increased in MHC-PPARβ/δ–HE hearts (2,155 ± 59 nmol/min/g dry wt) compared with controls (1,676 ± 151 nmol/min/g dry wt), whereas rates of palmitate oxidation were not significantly different (Figure 4B). Consistent with increased reliance on glucose as a cardiac substrate, myocardial glycogen levels were higher in MHC-PPARβ/δ mice than in controls (Figure 4C).
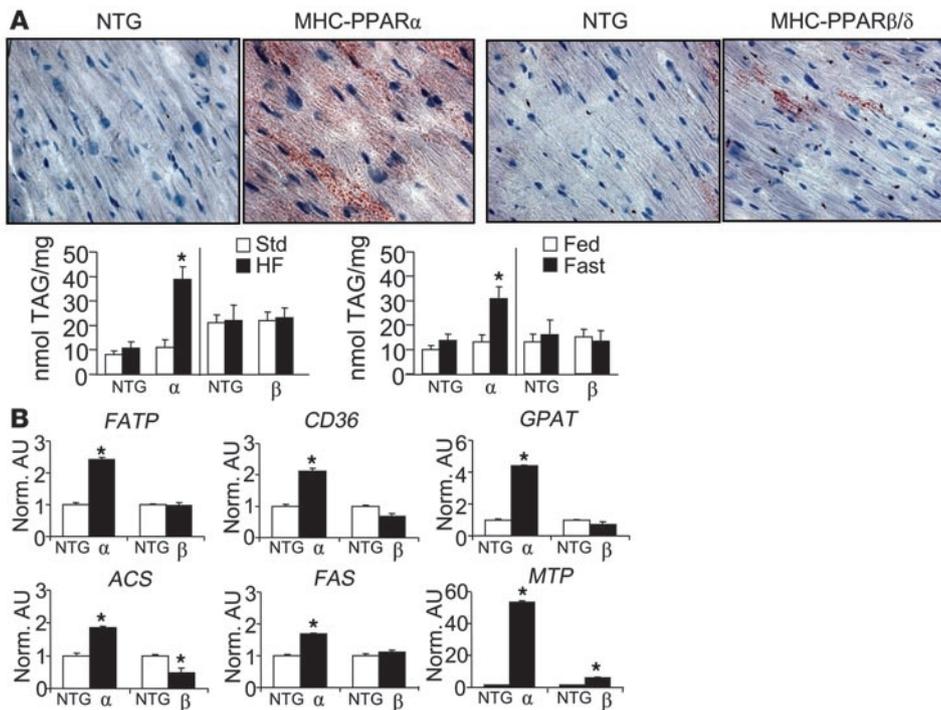
Figure 3
Diet-induced myocardial TAG accumulation in MHC-PPARα mice, but not MHC-PPARβ/δ mice. (**A**) Top: Histologic appearance of ventricular tissue samples from male MHC-PPARα–LE and MHC-PPARβ/δ–HE mice and NTG littermates after 4 weeks of HF diet. Red droplets indicate neutral lipid staining by oil red O. Bottom: Myocardial TAG levels determined by ESI/MS following HF diet or 48-hour fast in male MHC-PPARα and MHC-PPARβ/δ mice. (**B**) Mean ventricular mRNA levels for the indicated genes, as determined by RT-PCR analysis, shown as arbitrary units (AU) normalized to the value of NTG controls. RNA was isolated from mouse hearts after 4 weeks of HF diet. The *36B4* signal was used as internal normalization control. *P < 0.05 versus NTG.

PPARβ/δ and PPARα exert differential regulation on genes involved in cardiac glucose metabolism. The striking difference in myocardial glucose uptake and utilization in MHC-PPARβ/δ compared with MHC-PPARα mice prompted us to compare expression of genes involved in cardiac glucose metabolism. We previously found that the suppressive effects of PPARα on cardiac myocyte glucose utilization occurs at multiple levels including repression of the expression of genes involved in glucose import (*GLUT4*) and glycolysis (phosphofructokinase [*PFK*; *Pfk*]) (19, 20). In contrast, expression levels of genes encoding GLUT4 and PFK were significantly increased in hearts of MHC-PPARβ/δ mice compared with controls (Figure 5A). *GLUT1* (*Slc2a1*) gene expression was increased in MHC-PPARα mouse hearts, possibly as a compensatory response to the marked downregulation of *GLUT4* expression (Figure 5A). *GLUT1* gene expression was not significantly elevated in MHC-PPARβ/δ mouse hearts. Levels of hexokinase (HK; Hk2) mRNA were not significantly altered in either MHC-PPARα or MHC-PPARβ/δ mouse hearts (Figure 5A). These results are consistent with the substrate uptake and flux data and indicate that PPARβ/δ and PPARα exert distinct effects on gene regulatory programs involved in cardiac glucose metabolism.

Given that the PPAR isoform–specific gene regulatory patterns found in the transgenic lines could reflect an artificial pattern as a result of chronic nuclear receptor overexpression, we next assessed the effects of activating endogenous PPARα and PPARβ/δ in vivo. For these experiments, WT (B6CBAF1/J) mice were treated with the PPARα-specific agonist fenofibrate, the PPARβ/δ-specific agonist L-165,041, or vehicle (DMSO) for 3 days. As observed in the transgenic mice, treatment with either PPAR agonist resulted in increased cardiac expression of *MCAD*, a known PPAR target gene involved in mitochondrial FAO (Figure 5B). In contrast, mice treated with L-165,041 had increased myocardial *GLUT4* and *PFK* gene expression, whereas no increase was observed in mice treated with fenofibrate or vehicle (Figure 5B). Rather, fenofibrate treatment

led to a modest decrease in *GLUT4* and *PFK* mRNA levels. Consistent with the observed difference in myocyte TAG accumulation in the transgenic models, cardiac *CD36* gene expression (based on quantitative RT-PCR analysis) was induced by fenofibrate but not by L-165,041 (Figure 5B).

PPAR agonist studies were also performed with rat ventricular cardiac myocytes in culture to determine whether the observed differential metabolic and gene regulatory responses were mediated directly or via extracardiac effects. Myocytes were treated with fenofibrate, L-165,041, or vehicle for 48 hours, followed by analysis of gene expression and 2-deoxyglucose (2-DG) uptake rates. Consistent with the in vivo findings, basal and insulin-stimulated 2-DG uptake rates were increased in cells exposed to L-165,041 (Figure 5C), concomitant with increased *GLUT4* and *PFK* gene expression (Supplemental Figure 2), whereas no increase was observed in cells treated with DMSO or fenofibrate. As also predicted by the in vivo studies, both fenofibrate and L-165,041 activated *MCAD* and *M-CPT 1b* gene expression (Supplemental Figure 2). Collectively, these results demonstrate that PPAR isoform–specific agonists confer the same differential pattern of metabolic responses observed in hearts of MHC-PPARβ/δ and MHC-PPARα mice. Specifically, both PPARβ/δ and PPARα activated the FAO pathway, whereas activation of PPARβ/δ, but not PPARα, activated the glucose utilization pathway, and PPARα, but not PPARβ/δ, activated the FA uptake pathway.

Differential regulation of GLUT4 gene transcription by PPARβ/δ and PPARα. As an initial step toward characterizing the mechanism involved in the differential regulation of glucose metabolic genes by PPARβ/δ and PPARα, transfection studies were performed in cardiac ventricular myocytes in culture. For these studies, PPARβ/δ or PPARα expression vectors were cotransfected with a reporter plasmid containing a firefly luciferase gene driven by 2,240 bp of the WT human *GLUT4* gene promoter region (GLUT4.Luc.2240; Figure 6A) in the presence or absence of PPARα-specific (fenofibrate) or PPARβ/δ-specific (L-165,041) ligands. GLUT4.Luc.2240
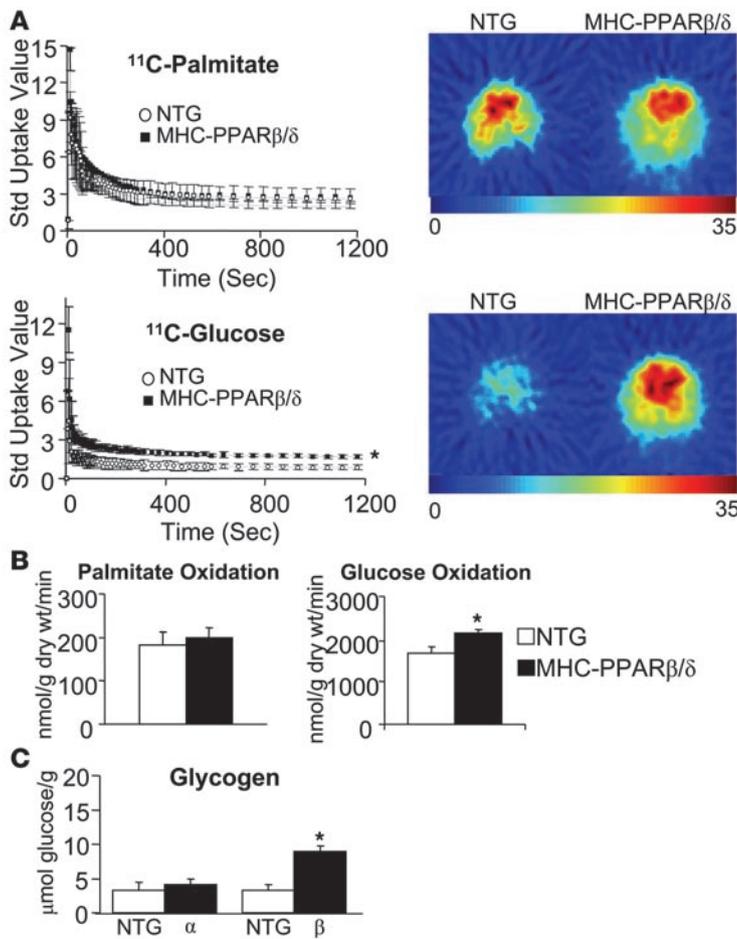
Figure 4
Increased myocardial glucose utilization in MHC-PPARβ/δ mice. (**A**) Left: Standardized uptake value time-activity curves for ^{11}C-palmitate and ^{11}C-glucose into female MHC-PPARβ/δ–HE and NTG hearts as determined by microPET. Values are mean ± SD. Right: Representative microPET images at 20 seconds after injection of ^{11}C-palmitate or ^{11}C-glucose. Images are normalized to total amount of radioactivity injected and body weight. The relative amounts of tracer uptake, ranging 0–35, are indicated by the color scale. (**B**) Oxidation of [9,10-^{3}H]palmitate and [U-^{14}C]glucose was assessed in isolated working hearts of 12-week-old male MHC-PPARβ/δ–HE and NTG control mice. Bars represent mean oxidation rates expressed as nanomoles substrate oxidized per gram dry mass per minute. (**C**) Glycogen levels were assessed in mouse hearts from male MHC-PPARα–LE and MHC-PPARβ/δ–HE mice and NTG controls. Results are presented as glucose released from glycogen and normalized to tissue weight. *$P < 0.05$ versus NTG.

activity was significantly repressed by PPARα in an exogenous ligand–independent manner (Figure 6B). In contrast, PPARβ/δ activated GLUT4.Luc.2240, an effect that was additive with L-165,041 treatment (Figure 6B). These results, which are consistent with the gene expression studies, demonstrate that PPARα and PPARβ/δ exert differential transcriptional regulatory effects on the GLUT4 gene. Interestingly, the PPARα-mediated repressive effect was not influenced by addition of exogenous activator, whereas the PPARβ/δ-mediated activation was additive with addition of L-165,041. These latter results suggest that endogenous ligand is limiting for PPARβ/δ and/or that the mechanism whereby PPARα exerts its repressive effect is ligand independent.

We have shown previously that a well-characterized myocyte enhancing factor 2a (MEF2a) site within the *GLUT4* promoter is necessary for the repressive effect of PPARα on GLUT4 transcription (28). To determine whether this regulatory site is required for the observed differential transcriptional regulation of GLUT4. Luc.2240 by PPARα and PPARβ/δ, cotransfection studies were repeated with a *GLUT4* promoter in which the MEF2a site was deactivated by site-directed mutagenesis (GLUT4.Luc.MEF_M; Figure 6A; ref. 28). The PPARα-mediated repressive effect and the PPARβ/δ-mediated activation were both abolished with GLUT4. Luc.MEF_M (Figure 6B), demonstrating that the differential transcriptional regulatory effects require the MEF responsive site.

MHC-PPARβ/δ mice are relatively resistant to myocardial ischemia/ reperfusion injury. Previous studies have shown that increased

rates of myocardial FAO and reduced rates of glucose utilization, as occur in the diabetic heart, sensitize the myocardium to ischemia/reperfusion (I/R) injury (17, 27, 29, 30). Given that the MHC-PPARβ/δ mice had increased capacity for myocardial glucose uptake and oxidation, we sought to determine whether they were resistant to I/R injury. To this end, MHC-PPARβ/δ, MHC-PPARα, and WT control mice were subjected to I/R injury by occluding the left anterior descending artery for 30 minutes, followed by 24 hours of reperfusion. Compared with NTG littermates, the hearts of MHC-PPARβ/δ mice exhibited significantly less I/R injury, as determined by measurement of infarcted area relative to area at risk (IA/AAR; 42.8% ± 3.5% versus 59.9% ± 6.8%; *P* < 0.05; Figure 7). In contrast, MHC-PPARα mice had increased IA/AAR compared with NTG littermates, although the difference was not statistically significant (52.6% ± 4.5% versus 48.3% ± 5.2%; Figure 7). The percent area at risk relative to the whole heart was not different between NTG and MHC-PPARα mice (42.4% ± 5.6% and 34.9% ± 3.7%) or between NTG and MHC-PPARβ/δ mice (49.6% ± 4.8% and 40.0% ± 3.6%; Supplemental Figure 3). Thus, as predicted by the myocardial fuel utilization pattern, MHC-PPARβ/δ mice are relatively protected against I/R injury.

Discussion
The normal postnatal mammalian heart exhibits remarkable fuel flexibility, switching between FA and glucose according to nutritional state, physical activity, and diurnal rhythms. This substrate
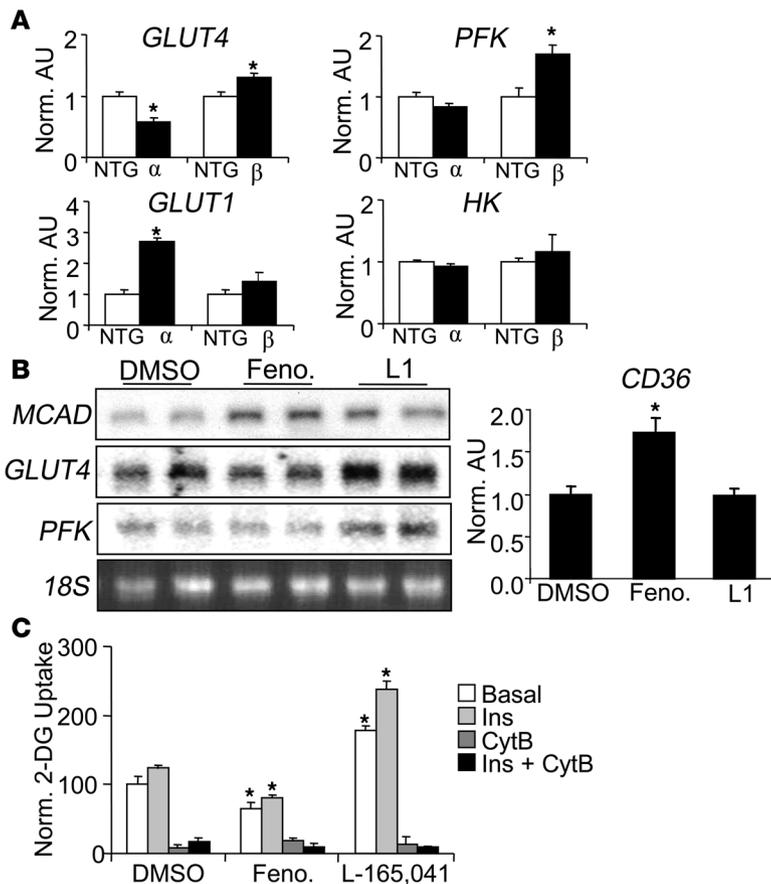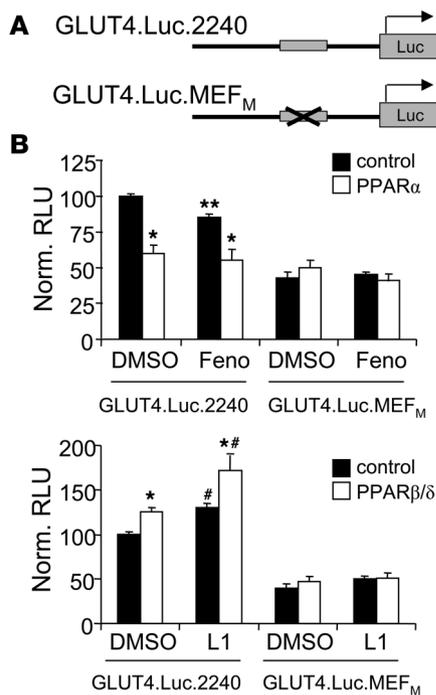
Figure 5
PPARα- and PPARβ/δ-specific ligands exert differential regulation on cardiac metabolic target genes. (**A**) Mean ventricular mRNA levels in MHC-PPARα and MHC-PPARβ/δ mice, as determined by RT-PCR analysis (corrected to *36B4* expression), shown as arbitrary units (AU) normalized to the value of NTG controls. (**B**) Representative autoradiographs of Northern blot (left) and RT-PCR (right) analyses performed with RNA isolated from hearts of WT mice treated with fenofibrate (Feno), L-165,041 (L1), or DMSO control for 3 days. (**C**) Rate of 2-DG uptake (mean ± SEM) determined in neonatal rat ventricular cardiomyocytes exposed to fenofibrate, L-165,041, or DMSO for 48 hours. Rates of 2-DG uptake were determined under basal, insulin-stimulated (Ins), or cytochalasin B–treated (CytB; to inhibit GLUT4) conditions. *$P < 0.05$ versus appropriate control.

flexibility is altered in myocardial disease states. For example, hypertensive heart disease is associated with reduced capacity for cardiac FA utilization (31–33). Conversely, the diabetic heart shifts toward increased reliance on lipid substrates, leading to excessive rates of myocardial FA uptake and oxidation, concomitant with reduced glucose utilization. Evidence is emerging that this loss of cardiac fuel flexibility contributes to the development of heart failure and sensitizes the heart to ischemic injury. The metabolic derangements of the diabetic heart involve gene regulatory programming via chronic activation of the nuclear receptor PPARα. We have shown previously that the cardiac phenotype of MHC-PPARα transgenic mice (19) is strikingly similar to the diabetic heart, providing evidence for a link between derangements in myocardial lipid and glucose metabolism and cardiac dysfunction. As described herein, the related nuclear receptor PPARβ/δ exerted remarkably different actions on cardiac metabolism, including versatility in fuel utilization associated with preservation of cardiac function.

Myocyte lipid accumulation is characteristic of the diabetic heart (34). The term *lipotoxicity* has been used to describe the toxic effects of excessive FA import on cellular function and viability (35). The diabetic heart exhibits increased FA uptake and myocyte lipid accumulation, ventricular hypertrophy and dysfunction, derangements in mitochondrial function, increased rates of myocyte apoptosis, and cardiomyopathy characterized by hypertrophy and diastolic/systolic ventricular dysfunction (36–39). The lipid metabolic derangements of the diabetic heart, as modeled by MHC-PPARα mice, underscore the impact of chronic PPARα-driven increases in myocardial FA uptake and utilization. It is believed that despite

increased capacity of diabetic and MHC-PPARα hearts to burn fat, FAO rates are insufficient to match the high rates of FA import and esterification, leading to diversion of FA intermediates to toxic pathways including peroxisomal oxidation and ceramide biosynthesis — both of which lead to the generation of cellular toxins (40). In this study, we describe the surprising finding that in contrast to MHC-PPARα mice, MHC-PPARβ/δ mice did not develop myocyte lipid accumulation or cardiomyopathy, even in the context of a HF diet. One likely explanation for this striking difference is that myocardial FA uptake and esterification rates were increased in MHC-PPARα mice but not in MHC-PPARβ/δ mice. The expression of genes involved in FA uptake (*FATP1* and *CD36*) and triglyceride synthesis (*GPAT*, *ACS*, *FAS*, and *MTP*) was activated in the hearts of MHC-PPARα mice but not in MHC-PPARβ/δ mice. This differential gene regulation was also noted when PPARα and PPARβ/δ agonists were administered to WT mice. Interestingly, genes involved in mitochondrial FAO were activated to similar levels in both transgenes. Collectively, these results suggest that the striking differences in cardiac lipid metabolic phenotype exhibited by PPARα compared with PPARβ/δ transgenic mice are related to differential activation of a subset of gene regulatory programs driving cellular transport and esterification of FA.

In 1963, Randle described the glucose-FA cycle (41). This seminal study demonstrated regulatory crosstalk between the 2 major fuel utilization pathways in the heart. Specifically, increased flux through the FAO pathway generates intermediates that confer reciprocal allosteric repressive effects on the pyruvate dehydrogenase complex, leading to a reduction in glucose oxidation. The

Figure 6
PPARβ/δ and PPARα differentially regulate *GLUT4* gene transcription through a MEF2a-responsive region in the *GLUT4* promoter. (**A**) *GLUT4* promoter reporter constructs (GLUT4.Luc.2240 and GLUT4.Luc.MEF_M) were cotransfected into rat neonatal ventricular cardiomyocytes with a PPARα or PPARβ/δ expression vector (pBOS-PPARα or pCMX-PPARβ/δ) or empty vector control. Cells were exposed for 48 hours with fenofibrate, L-165,041, or DMSO control. The GLUT4.Luc.MEF_M promoter reporter construct is crossed out to indicate that the MEF2a binding site has been deactivated by site-directed mutagenesis. (**B**) Luciferase activity (mean ± SEM) shown as relative luciferase units (RLU) corrected for β-galactosidase activity and normalized to the value of empty expression vector–transfected cells (*n* = 12). *P < 0.05 versus empty vector control; **P < 0.01 versus DMSO; #P < 0.05 versus DMSO.

repression of glucose oxidation by high rates of FAO described by Randle is one likely mechanism whereby myocardial glucose utilization is reduced in the diabetic heart. In addition, the capacity for glucose import is constrained in the diabetic heart, which is related, at least in part, to decreased insulin-stimulated translocation of GLUT4. Evidence is emerging that reduced rates of glucose oxidation contribute to diabetic cardiac dysfunction, particularly in the setting of I/R injury (17, 27, 29, 30). Previously we have shown that the PPARα-driven increase in myocardial FAO rates in MHC-PPARα mice is linked to diminished rates of glucose uptake and oxidation and reduced expression of the genes encoding GLUT4 and the glycolytic enzyme PFK (19). This regulatory crosstalk at the gene expression level is analogous to the rapid posttranslational control of the Randle cycle. In striking contrast to MHC-PPARα mice, MHC-PPARβ/δ mice exhibited increased rates of myocardial glucose uptake and utilization. These observations are consistent with the results of recent studies by others demonstrating that PPARβ/δ promotes insulin sensitivity in muscle and liver (42, 43). Our results also demonstrate that, as predicted by the observed increased capacity for myocardial glucose utilization, the hearts of MHC-PPARβ/δ mice are resistant to I/R injury.

In addition to PPARα and PPARβ/δ, the heart also expresses low levels of PPARγ. Recently, the development and characterization of mice with cardiac-specific overexpression of PPARγ (MHC-PPARγ) have been described previously (44). Similar to MHC-PPARα mice,

MHC-PPARγ mice have increased expression of *CD36*, myocyte lipid accumulation, increased myocardial uptake, and cardiomyopathy (44). This phenotype is similar to that of MHC-PPARα mice (19, 20). However, unlike MHC-PPARα mice, myocardial *GLUT4* mRNA levels and 2-DG uptake are upregulated in the high-expressing line of MHC-PPARγ mice, a pattern similar to that of the MHC-PPARβ/δ mice reported here. Together, these findings suggest that PPARγ shares gene regulatory targets and metabolic responses in heart with both PPARα and PPARβ/δ. It will be of significant interest to delineate shared cardiac PPARα and PPARγ gene targets that are distinct from that of PPARβ/δ.

The observation that MHC-PPARβ/δ hearts utilize glucose at high rates prompted us to investigate the expression of genes involved in this pathway. In contrast to the repressive effects of

Figure 7
MHC-PPARβ/δ mice are resistant to myocardial I/R injury. Top: Representative cross-sectional images of the heart after I/R injury followed by staining with TTC and Evans blue as described in Methods. Blue staining represents uninjured tissue; orange represents area at risk; white represents the infarcted region. S, ventricular septum. Bottom: IA/AAR (mean ± SEM) for male and female MHC-PPARα–LE and MHC-PPARβ/δ–HE mice and corresponding NTG littermates (*n* ≥ 15 per group). *P < 0.05 versus NTG.
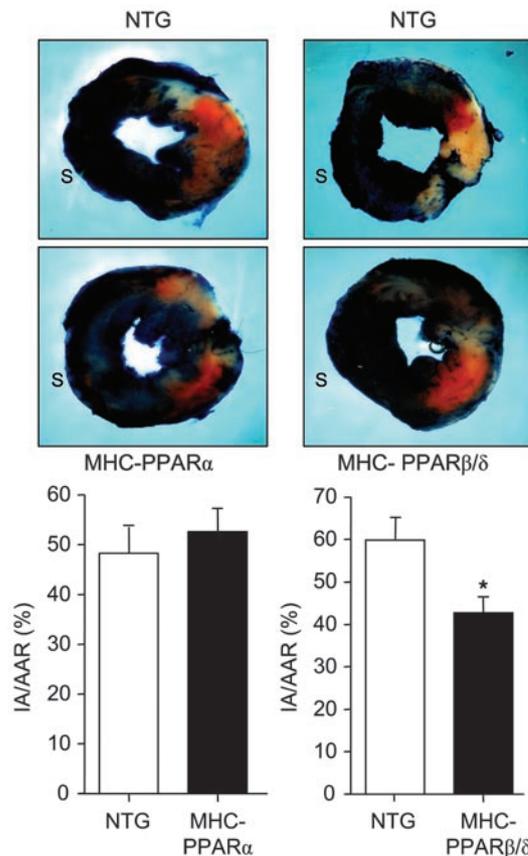
PPARα, we found that PPARβ/δ induced the expression of genes encoding GLUT4 (glucose transport) and PFK (glycolysis) in the MHC-PPARβ/δ heart. These results do not reflect an artifact of overexpression, given that the same patterns were observed in vivo and in cultured myocytes using ligand activation of the endogenous receptors. To gain further insight into this mechanism, we focused on the reciprocal regulation of *GLUT4* gene expression by PPARα and PPARβ/δ. As predicted by the results of the gene expression studies, we found that PPARβ/δ and PPARα exerted differential transcriptional regulation of a *GLUT4* gene promoter-reporter, an effect that requires a well-characterized MEF2a response element rather than a PPAR-responsive element. Indeed, our analysis of the DNA sequence in the *GLUT4* gene 5′-flanking region did not reveal a PPAR recognition sequence. Collectively, these findings define one mechanism whereby PPAR isotypes exert differential regulation on a shared target gene. Future studies will be necessary to determine whether this is a general paradigm applicable to other differentially regulated targets, including those involved in FA uptake and esterification.

Significant evidence supports the notion that therapeutic strategies aimed at reducing myocardial FA uptake and oxidation, while increasing glucose utilization, will improve the function of the diabetic heart under basal conditions and following ischemic insult. We show here that in the setting of myocardial I/R injury, cardiac-specific overexpression of PPARβ/δ was cardioprotective: infarct sizes were smaller in the MHC-PPARβ/δ mice compared with WT or MHC-PPARα mice. Interestingly, we have found that expression of PPARα, but not PPARβ/δ, is activated in mouse models of type 2 diabetes, indicating that the ratio of myocardial PPARα to PPARβ/δ is increased in this disease state (our unpublished observations). Accordingly, selective activation of *PPAR*β/δ shows promise as a therapeutic strategy for diabetic cardiac dysfunction if the same proves true in humans.

Methods

Materials. The PPARα-specific agonist fenofibrate was obtained from Sigma-Aldrich. The PPARβ/δ-specific agonist L-165,041 was obtained from Calbiochem.

*Generation of MHC-PPAR*β/δ *mice*. A cDNA construct containing a 1.0-kb PPARβ/δ cDNA was cloned downstream of the cardiac α-MHC promoter (clone 26; gift of J. Robbins, The Children's Hospital Research Foundation, Cincinnati, Ohio, USA). Transgenic mice were generated by microinjection of the MHC-PPARβ/δ construct into fertilized 1-cell C57BL/6 × CBA/J F$_1$ embryos in the Washington University Mouse Genetics Core.

Animal studies. Cardiac functional and metabolic end points were analyzed in male and female pairs of MHC-PPARβ/δ and littermate NTG mice (25–30 g body weight) ranging in age from 8 to 16 weeks. The majority of data presented in this manuscript represents studies with male mice, with exceptions noted in the figure legends. In each case, independent analyses of the opposite gender gave identical results (data not shown). For diet studies, mice were allowed ad libitum access to HF chow, which provides 43% of the calories from fat (TD 97268; Harlan Teklad). For fasting studies, mice were housed in individual cages at the start of each experiment and fasted for 48 hours. Control mice were allowed ad libitum access to standard laboratory rodent chow (diet 5053; Purina Mills Inc.). For agonist studies, mice were treated with DMSO, fenofibrate (100 mg/kg/d), or L-165,041 (10 mg/kg/d) by oral gavage once daily for 3 days. All animal studies were conducted in strict accordance with the NIH guidelines for humane treatment of animals and were approved by the Animal Studies Committee at Washington University School of Medicine.

Mouse isolated working heart preparation. Mouse working heart perfusions were performed as previously described (27). Briefly, isolated working hearts were perfused with Krebs-Henseleit solution containing 5 mM glucose, 100 μU/ml insulin, and 0.4 mM palmitate. Myocardial FA and glucose oxidation rates were determined by quantitative collection of ^{3}H$_2$O or ^{14}CO$_2$ produced by hearts perfused with buffer containing [9,10-^{3}H]palmitate or [U-^{14}C]glucose.

Isolated neonatal rat ventricular cardiomyocytes. Neonatal rat ventricular cardiomyocytes were isolated as previously described (45); stimulated with DMSO, 1 μM fenofibrate, or 10 μM L-165,041 for 48 hours; and subjected to RNA isolation for Northern blot analysis or assayed for 2-DG uptake rates.

2-DG uptake assay. 2-DG uptake rates were determined in isolated neonatal rat ventricular cardiomyocytes that were stimulated with DMSO, fenofibrate (1 μM), or L-165,041 (10 μM) for 48 hours. Five hours prior to the experiment, cells were placed in serum-free medium (Optimem; Invitrogen). One hour prior to the experiment, 1 U/ml insulin (Sigma-Aldrich) and 10 μM cytochalasin B (Sigma-Aldrich) were added to intended wells. Cells were incubated for 10 minutes with uptake solution (pH 7.4) containing [^{3}H]2-DG (2 mCi/ml; American Radiolabeled Nucleotides), 10 μM 2-DG, 140 mM NaCl, 20 mM HEPES, 5 mM KCl, 2.5 mM MgSO$_4$, and 1 mM CaCl$_2$. The reaction was stopped with ice-cold PBS, cells were lysed with 50 mM NaOH, lysates were counted by scintillation, and rates of 2-DG uptake were calculated.

MicroPET studies. Prior to the imaging session, mice were individually housed and semifasted overnight (allowed access to 1 pellet of rodent chow). The next morning, mice were fasted for an additional 3 hours before experiments were performed. MicroPET imaging of ^{11}C-palmitate and 1-^{11}C-glucose uptake and metabolism was performed on the Focus 120 and 220 (Concord microPET Systems) as previously described (19). Briefly, regions of interest were placed on the heart of each mouse using the palmitate image as landmark. Regions of interest were normalized to animal weight and activity injected to obtain dynamic standardized uptake value time activity curves. NTG and MHC-PPARβ/δ dynamic standardized uptake values were grouped and averaged. MicroPET images were similarly standardized.

Echocardiographic studies. Transthoracic M-mode and 2-dimensional echocardiography was performed on conscious mice in the Washington University Mouse Cardiovascular Phenotyping Core using an Acuson Sequoia 256 Echocardiography system (Acuson Corp.) as described previously (46).

RNA analyses. Total RNA was isolated from mouse cardiac ventricles using the RNAzol method (Tel-Test). Northern blot analysis was performed with QuikHyb (Stratagene) using random-primed ^{32}P-labeled cDNA clones. Band intensities were quantified using a STORM Phosphorimager (GE Healthcare) and normalized to the expression of 36B4 using ImageQuaNT5.2 software. Real-time quantitative RT-PCR was performed using the ABI Prism 7500 Sequence Detection System and reagents supplied by Applied Biosystems. Signal intensity was normalized to expression of 36B4.

Immunoblotting studies. Total cardiac protein was prepared as previously described (47). Western blot analyses were performed using a rabbit polyclonal PPARβ/δ (H-74) antibody (Santa Cruz Biotechnology Inc.) and a rabbit polyclonal anti-GLUT4 antibody (gift of M. Mueckler, Washington University School of Medicine). Detection was performed by measuring the chemiluminescent signal as assayed by SuperSignal Ultra (Pierce).

Histologic analyses. Mouse hearts were collected, and a midventricular cross-sectional slice of myocardium was immersed in Tissue-Tek OCT Compound (Sakura Finetek USA Inc.) and snap-frozen using Cytocool II (Richard-Allan Scientific) in a cryomold for sectioning. Sections were stained with oil red O to detect intracellular neutral lipid accumulation.

Myocardial TAG levels. ESI/MS was used to quantitate myocardial TAG levels as previously described (48). Briefly, lipids were extracted from mouse hearts using a modified Bligh and Dyer technique, and subsequent analysis of TAG species was performed in the positive ion mode.

Glycogen measurements. Mouse cardiac tissue from 8-week-old male and female MHC-PPARβ/δ and NTG mice was pulverized under liquid nitrogen and homogenized in a 0.3 M perchloric acid solution. The muscle extract was then assayed with and without amyloglucosidase digestion (Sigma-Aldrich) in 50 mM sodium acetate (pH 5.5) and 0.02% BSA. Resulting changes in absorption at 340 nM were compared with a standard of 0–80 μmol glucose. Results are presented as glucose released from glycogen and normalized to tissue weight.

Promoter studies. GLUT4 promoter reporter constructs (GLUT4.Luc.2240; kindly provided by J. Pessin, University of Iowa, Iowa City, Iowa, USA; and GLUT4.Luc.MEF$_M$) were cotransfected into rat neonatal ventricular cardiomyocytes with a PPARα or PPARβ/δ expression vector (pBos-PPARα or pCMX-PPARβ/δ) or empty vector control (pEFBOS or pCMX). Cells were stimulated for 48 hours with PPARα-specific (fenofibrate) or PPARβ/δ-specific (L-164,041) agonists or DMSO control. Luciferase activity in relative luciferase units was corrected for SV 40 β-galactosidase (500 ng/ml) and normalized to the value of empty vector control–transfected cells.

Myocardial I/R studies. Mice were anesthetized (ketamine/xylazine), surgically prepped and ventilated on a Harvard rodent respirator. After exposing the heart, the pericardium was removed, and a 9-0 polypropylene suture with a U-shaped needle was passed under the left anterior descending artery. The suture was tied over a piece of PE-10 tubing to occlude the left anterior descending artery for 30 minutes. After the occlusion period, the PE-10 tube was carefully removed to allow for reperfusion. The chest was then closed and the mouse recovered. After 24 hours of reperfusion, the mouse was again anesthetized and injected subcutaneously with heparin (1 U/g). The abdominal cavity was opened, and a heparin/KCL mixture was injected into the inferior vena cava to stop the heart. The mouse was then bled out by cutting the renal artery. The carotid arteries were ligated, the descending aorta was cannulated, and the heart was perfused with a phosphate buffer followed by 1% TTC (Fisher). The left anterior descending artery was then reoccluded at the original site, and 1% Evans Blue Dye (Sigma-Aldrich) was perfused. The heart was removed and frozen at –20°C for 1 hour, sliced into 5 pieces, and fixed in 4% neutral buffered formalin overnight at 4°C. After 24 hours in formalin, the heart slices were weighed. An image of each side of all slices was taken using a Canon Power Shot A80 digital camera. Each image was analyzed using the Image Tool software (UTHSCSA). The areas were quantified by averaging both sides of each slice and normalizing to slice weight. Next, a region at risk was calculated as the portion of the LV absent of blue dye. The percent of infarcted tissue (white area) within this region of risk was calculated (see Figure 7).

Statistics. Data were analyzed by 2-tailed Student's *t* test or ANOVA and presented as mean ± SEM. A *P* value less than 0.05 was considered statistically significant.

Address correspondence to: Daniel P. Kelly, Center for Cardiovascular Research, Washington University School of Medicine, 660 S. Euclid Ave., Campus Box 8086, St. Louis, Missouri 63110, USA. Phone: (314) 362-8908; Fax: (314) 362-0186; E-mail: dkelly@im.wustl.edu.

1. Zimmet, P., Alberti, K.G., and Shaw, J. 2001. Global and societal implications of the diabetes epidemic. *Nature.* **414**:782–787.
2. Wilson, P.W. 1998. Diabetes mellitus and coronary heart disease. *Am. J. Kidney Dis.* **32**:S89–S100.
3. Wilson, P.W., D'Agostino, R.B., Parise, H., Sullivan, L., and Meigs, J.B. 2005. Metabolic syndrome as a precursor of cardiovascular disease and type 2 diabetes mellitus. *Circulation.* **112**:3066–3072.
4. Stamler, J., Vaccaro, O., Neaton, J.D., and Wentworth, D. 1993. Diabetes, other risk factors, and 12-yr cardiovascular mortality for men screened in the Multiple Risk Factor Intervention Trail. *Diabetes Care.* **16**:434–444.
5. Jaffe, A.S., et al. 1984. Increased congestive heart failure after myocardial infarction of modest extent in patients with diabetes mellitus. *Am. Heart J.* **108**:31–37.
6. Abbott, R.D., Donahue, R.P., Kannel, W.B., and Wilson, P.W. 1988. The impact of diabetes on survival following myocardial infarction in men vs. women. *JAMA.* **260**:3456–3460.
7. Manson, J.E., et al. 1991. A prospective study of maturity-onset diabetes mellitus and risk of coronary heart disease and stroke in women. *Arch. Intern. Med.* **151**:1141–1147.
8. Miettinen, H., et al. 1998. Impact of diabetes on mortality after the first myocardial infarction. The FINMONICA Myocardial Infarction Register Study Group. *Diabetes Care.* **21**:69–75.
9. Cho, E., Rimm, E.B., Stampfer, M.J., Willett, W.C., and Hu, F.B. 2002. The impact of diabetes mellitus and prior myocardial infarction on mortality from all causes and from coronary heart disease in men. *J. Am. Coll. Cardiol.* **40**:954–960.
10. Bing, R.J., Siegel, A., Ungar, I., and Gilbert, M. 1954. Metabolism of the human heart. II. Studies on fat, ketone and amino acid metabolism. *Am. J. Med.* **16**:504–515.
11. Taegtmeyer, H., Wilson, C., Razeghi, P., and Sharma, S. 2005. Metabolic energetics and genetics in the heart. *Ann. N. Y. Acad. Sci.* **1047**:208–218.
12. Paulson, D.J., and Crass, M.F. 1982. Endogenous triacylglycerol metabolism in diabetic heart. *Am. J. Physiol.* **242**:H1084–H1094.
13. Taegtmeyer, H., McNulty, P., and Young, M.E. 2002. Adaptation and maladaptation of the heart in diabetes: Part I General Concepts. *Circulation.* **105**:1727–1733.
14. Young, M.E., McNulty, P., and Taegtmeyer, H. 2002. Adaptation and maladaptation of the heart in diabetes: Part II Potential Mechanisms. *Circulation.* **105**:1861–1870.
15. Frustaci, A., et al. 2000. Myocardial cell death in human diabetes. *Circ. Res.* **87**:1123–1132.
16. Boudina, S., et al. 2005. Reduced mitochondrial oxidative capacity and increased mitochondrial uncoupling impair myocardial energetics in obesity. *Circulation.* **112**:2686–2695.
17. Lopaschuk, G.D. 1989. Alterations in myocardial fatty acid metabolism contribute to ischemic injury in the diabetic. *Can. J. Cardiol.* **5**:315–320.
18. Taegtmeyer, H. 2000. Metabolism--the lost child of cardiology. *J. Am. Coll. Cardiol.* **36**:1386–1388.
19. Finck, B., et al. 2002. The cardiac phenotype induced by PPARα overexpression mimics that caused by diabetes mellitus. *J. Clin. Invest.* **109**:121–130.
20. Finck, B., et al. 2003. A critical role for PPARα-mediated lipotoxicity in the pathogenesis of diabetic cardiomyopathy: Modulation of phenotype by dietary fat content. *Proc. Natl. Acad. Sci. U. S. A.* **100**:1226–1231.
21. Desvergne, B., and Wahli, W. 1999. Peroxisome proliferator-activated receptors: Nuclear control of metabolism. *Endocr. Rev.* **20**:649–688.
22. Huss, J.M., and Kelly, D.P. 2004. Nuclear receptor signaling and cardiac energetics. *Circ. Res.* **95**:568–578.
23. Herrero, P., et al. 2006. Increased myocardial fatty acid metabolism in patients with type 1 diabetes mellitus. *J. Am. Coll. Cardiol.* **47**:598–604.
24. Welch, M.J., et al. 2006. Assessment of myocardial metabolism in diabetic rats using small-animal PET: A feasible study. *J. Nucl. Med.* **47**:689–697.
25. Gilde, A.J., et al. 2003. PPARα and PPARβ/δ, but not PPARγ, modulate the expression of genes involved in cardiac lipid metabolism. *Circ. Res.* **92**:518–524.
26. Cheng, L., et al. 2004. Cardiomyocyte-restricted peroxisome proliferator-activated receptor-δ deletion perturbs myocardial fatty acid oxidation and leads to cardiomyopathy. *Nat. Med.* **10**:1245–1250.
27. Sambandam, N., et al. 2006. Chronic activation of PPARα is detrimental to cardiac recovery following ischemia. *Am. J. Physiol. Heart Circ. Physiol.*

290:H87–H95.

28. Finck, B.N., et al. 2005. A potential link between muscle peroxisome proliferator-activated receptor α signaling and obesity-related diabetes. *Cell Metab.* **1**:133–144.

29. Tian, R., and Abel, E.D. 2001. Responses of GLUT4-deficient hearts to ischemia underscore the importance of glycolysis. *Circulation.* **103**:2961–2966.

30. Taegtmeyer, H. 2005. Glucose for the heart: too much of a good thing? *J. Am. Coll. Cardiol.* **46**:49–50.

31. Huss, J.M., and Kelly, D.P. 2005. Mitochondrial energy metabolism in heart failure: A question of balance. *J. Clin. Invest.* **115**:547–555.

32. Russell, L.K., Finck, B.N., and Kelly, D.P. 2005. Mouse models of mitochondrial dysfunction and heart failure. *J. Mol. Cell. Cardiol.* **38**:81–91.

33. de las Fuentes, L., et al. 2003. Myocardial fatty acid metabolism: independent predictor of left ventricular mass in hypertension and in left ventricular dysfunction. *Hypertension.* **41**:83–87.

34. Finck, B., and Kelly, D.P. 2002. Peroxisome proliferator-activated receptor α (PPARα) signaling in the gene regulatory control of energy metabolism in the normal and diseased heart. *J. Mol. Cell. Cardiol.* **34**:1249–1257.

35. Unger, R.H. 2005. Longevity, lipotoxicity and leptin: the adipocyte defense against feasting and famine. *Biochimie.* **87**:57–64.

36. Chiu, H.-C., et al. 2001. A novel mouse model of lipotoxic cardiomyopathy. *J. Clin. Invest.* **107**:813–822.

37. Dyntar, D., et al. 2001. Glucose and palmitic acid induce degeneration of myofibrils and modulate apoptosis in rat adult cardiomyocytes. *Diabetes.* **50**:2105–2113.

38. Shen, X., et al. 2004. Cardiac mitochondrial damage and biogenesis in a chronic model of type I diabetes. *Am. J. Physiol. Endocrinol. Metab.* **287**:E896–E905.

39. Chiu, H.-C., et al. 2005. Transgenic expression of FATP1 in the heart causes lipotoxic cardiomyopathy. *Circ. Res.* **96**:225–233.

40. Okere, I.C., et al. 2006. Differential Effects of Saturated and Unsaturated Fatty Acid Diets on Cardiomyocyte Apoptosis, Adipose Distribution, and Serum Leptin. *Am. J. Physiol. Heart Circ. Physiol.* **291**:H38–H44.

41. Randle, P.J., Hales, C.N., and Garland, P.B. 1963. The glucose fatty-acid cycle. Its role in insulin sensitivity and the metabolic disturbances of diabetes mellitus. *Lancet.* **1**:785–789.

42. Barish, G.D., Narkar, V.A., and Evans, R.M. 2006. PPAR delta: a dagger in the heart of the metabolic syndrome. *J. Clin. Invest.* **116**:590–597.

43. Lee, C.H., et al. 2006. PPARδ regulates glucose metabolism and insulin sensitivity. *Proc. Natl. Acad. Sci. U. S. A.* **103**:3444–3449.

44. Son, N.-H., et al. 2007. Cardiomyocyte expression of PPARγ leads to cardiac dysfunction in mice. *J. Clin. Invest.* **117**:2791–2801.

45. Disch, D.L., et al. 1996. Transcriptional control of a nuclear gene encoding a mitochondrial fatty acid oxidation enzyme in transgenic mice: role for nuclear receptors in cardiac and brown adipose expression. *Mol. Cell. Biol.* **16**:4043–4051.

46. Tanaka, N., et al. 1996. Transthoracic echocardiography in models of cardiac disease in the mouse. *Circulation.* **94**:1109–1117.

47. Cresci, S., Wright, L.D., Spratt, J.A., Briggs, F.N., and Kelly, D.P. 1996. Activation of a novel metabolic gene regulatory pathway by chronic stimulation of skeletal muscle. *Am. J. Physiol.* **270**:C1413–C1420.

48. Han, X., Yang, K., Yang, J., Cheng, H., and Gross, R.W. 2006. Shotgun lipidomics of cardiolipin molecular species in lipid extracts of biological samples. *J. Lipid Res.* **47**:864–879.